EFFECT OF GEOMETRICAL STRUCTURE OF EMBEDDED PHASE CHANGE MATERIAL ON THE POWER GENERATION OF THERMOELECTRIC MODULE

Anbang-Liu, Zihua-Wu*, Huaqing-Xie, Yuanyuan-Wang,

Jianhui-Mao, Jiaojiao-Xing, Yihuai-Li

School of Environmental and Materials Engineering, College of Engineering, Shanghai Polytechnic University, Shanghai, 201209, P. R. China

E-mail: xiaobangzhiwang@qq.com (1st author E-mail address)

Abstract: *The effect of geometrical structure of embedded phase change material (PCM) on the power generation of the thermoelectric module (TEM) was studied in this work. Paraffin wax with different geometrical structure was embedded in a polymer container which is adhered to the hot junction of the fabricated TEM. Since the PCM can used as the heat source and provide latent heat when the heat source stops providing heat, applying the PCM in the TEM is an efficiency method to enhance the power generation of the TEM. Our experimental results show that the energy harvesting time becomes 60 seconds longer in comparison with the case without the PCM when 4.3 gram weight of paraffin wax is applied. At the same time, the power generation of the TEM increases by magnitude of 25%. Moreover, the output voltage and electrical energy generation of TEM with PCM increase with increasing both cross-area and height of the applied PCM.*

Keywords: Thermoelectric module; Phase change material;

1.Introduction

Thermoelectric module (TEM) is a solid-state device which converts heat to electricity directly and vise verse through the Seebeck effect. It works like heat engines, but is less bulky, reliable, has no moving parts and low operating cost [1-3]. In consideration of these advantages, TEM is promising to apply in the industry in order to convert waste heat into electricity. For example, it is used as automotive thermoelectric generator to increase fuel efficiency indirectly in the automobile field [4,5].

TEM is comprised of a hot lead and a cold lead, together with a single thermoelectric leg. A temperature gradient exists between the hot and cold ends, which enables TEM to generate electricity [6-8]. TEM conversion efficiency is determined by the thermoelectric properties of

*Corresponding Author's E-mail: wuzihua@sspu.edu.cn

the composed materials and the structure of the device. Among these two factors, the properties of thermoelectric material is determined by the dimensionless thermoelectric figure of merit ($ZT=\sigma S^2\kappa^{-1}T$, where S is the Seebeck coefficient, σ is the electrical conductivity, κ is the thermal conductivity and T is the temperature) [9,10]. To enhance ZT, a high Seebeck coefficient together with a high electrical conductivity and a low thermal conductivity is pursued. At the same time, modified structure of TEM is another important way to enhance the conversion efficiency of the TEM [11,12]. Unfortunately, the majority part of the heat fails to be converted into electricity due to a large amount of heat emissions, resulting in energy waste. Furthermore, the waste heat emissions have discontinuity and instability problems in time and space [13], such as the case that the TEM is applied in the automobile engine for energy harvesting. To solve these problems, a solution is proposed by using phase change material (PCM) to reuse dissipated heat [14]. By combining TEM with the PCM, the superfluous heat emitted from the heat source may store in PCM. Once the heat source was removed, the stored heat energy in PCM could support TEM to generate electricity.

So far, several literatures have paid close attention to the power generation properties of TEM with PCM applied. Samson *et al.* reported a specific aircraft thermoelectric generator, which consists of a phase change material attached to one side of the thermoelectric generator [15]. Yoon *et al.* demonstrated an impact-triggered thermoelectric generator (IT-TEG) that takes the latent heat released from crystallization of supersaturated sodium acetate trihydrate (SSAT) as heat source [16]. A single IT-TEG could generate a maximum instantaneous power of 2.08 mW in the process of SSAT's phase change transition. Jo *et al.* proposed a thermoelectric generator which was embedded with phase change materials for harvesting wasted heat energy [17]. The experimental results showed that the thermoelectric generator could continue generate electrical energy when the heat source was removed by the heat energy stored in the PCM. Elefsiniotis *et al.* designed an energy harvesting device used in high temperature condition with an organic PCM used as the heat source [18]. The harvest energy can reach a maximum value of 81.4 J. Zhang *et al.* utilized a thermoelectric generator to harvest solar and ambient energy [19−21]. A prototype work unit composed of a thermoelectric generator and phase change materials had been put into practice. Through the integrated use of their advantages, the system was designed to work continuously. All of the works above have proved that the application of PCM is an efficient method to increase the power generation in the TEM. Nevertheless, there is a lack of thinking about the influence of the geometrical structure of embedded PCM to the convert efficiency of the TEM. Therefore, in this study, the power generation properties of TEM embedded with PCM which have different cross-sectional diameter and height was studied in detailed. In section 2 and section 3, we present our experimental design and discuss experimental results, respectively. Finally, we conclude this study in section 4.

2.Design and methods

Among various PCMs, paraffin wax whose density 'ρ' is 0.76 g/cm^3 and specific heat capacity 'c' is 2.4 J/g·°C, as a kind of conventional phase change material, was used in this study. Paraffin wax has a large latent heat of fusion of about 173 kJ • kg^{-1} and a low melting point of less than 55 °C. These physical properties make it possible to store large amounts of

heat during the phase transition process [22]. Moreover, paraffin wax has advantages of low cost and very low volume change during melting.

The experimental setup can be found in Fig. 1 (a). It is composed of thermoelectric module (TEM), vacuum pump, power control equipment, data processing device, and data acquisition unit. The TEM is shown in Fig. 1 (b). The TEM uses a single thermoelectric leg with a diameter of 5 mm and a length of 20 mm. The PCM is filled in a cuboid polymer container with the height of 15 mm and the side length of 40 mm. The interior of the polymer container has a cylindrical space. In the center of cylindrical space, an aperture is provided to place the thermoelectric leg. The temperature is measured by using precision K-type thermocouples. The temperature of the heat source is controlled by power control equipment. The output voltage of TEM is measured by a data acquisition unit (Agilent data collector 34970A). In this study, to investigate the effect of the geometrical structure of embedded PCM on the power generation of the TEM, two types of structures of the PCM were set up and named as group A and group B. In group A, the height of PCM was fixed at 8 mm, and

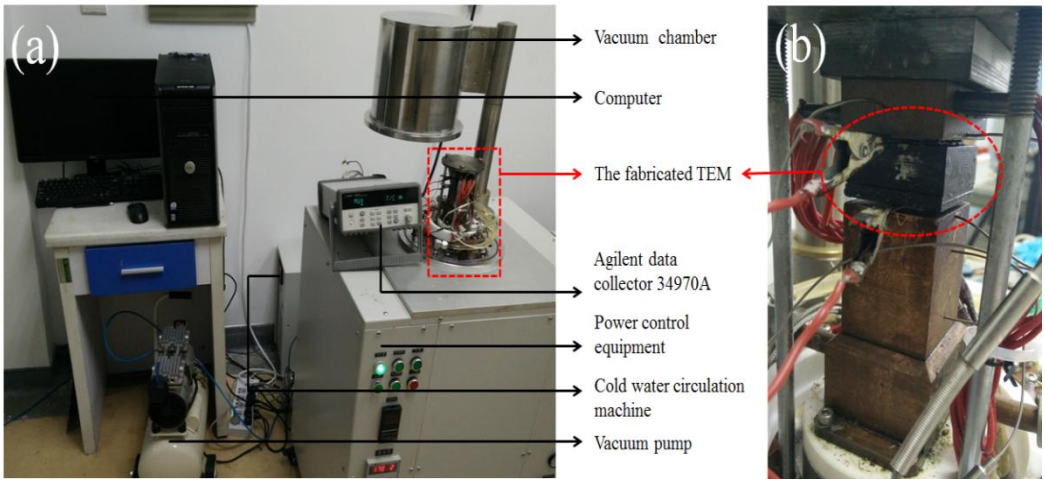

Fig. 1. (a) The experimental setup; (b) The fabricated TEM.

the circular cross-sectional diameter was set to be 24, 26, 30 mm, respectively. In group B, the circular cross-sectional diameter was fixed at 30 mm, and the height of PCM was set to be 2, 4, 8 mm, respectively.

Fig. 2 gives the schematic figure of the TEM. The experimental process was operated in a vacuum environment. On the top side of TEM, the electrical connection for single thermoelectric leg is defined as the hot junction and keeps in thermal contact with heat source. The embedded PCM is adhered to the hot junction. The temperature of heat source was fixed to be 60 °C. The bottom side of TEM assembly with circulating cold water is defined as the cold junction. The temperature of circulating cold water is set to be 15 °C. The thermoelectric leg extends vertically through the polymer container and PCM.

When the heat source begins to supply heat energy, the temperature of PCM will be increases. A large amount of heat energy was stored in the PCM during the phase change from solid to liquid. Since the thermal resistance between PCM and TEM is much larger than that between heat source and TEM, the hot junction temperature of TEM is under control of

heat source without being interfered by other factors. When the heat source stops supplying heat, the PCM is operated as a heat source since the heat released from PCM is much larger than the energy stored by the polymer container. Therefore, the hot junction temperature of TEM is mainly determined by the melting point and the latent heat of PCM when the heat source stops supplying heat. This makes it possible that the TEM could generate electricity continuously in a short period when the heat supply is insufficient or the heat source is removed.

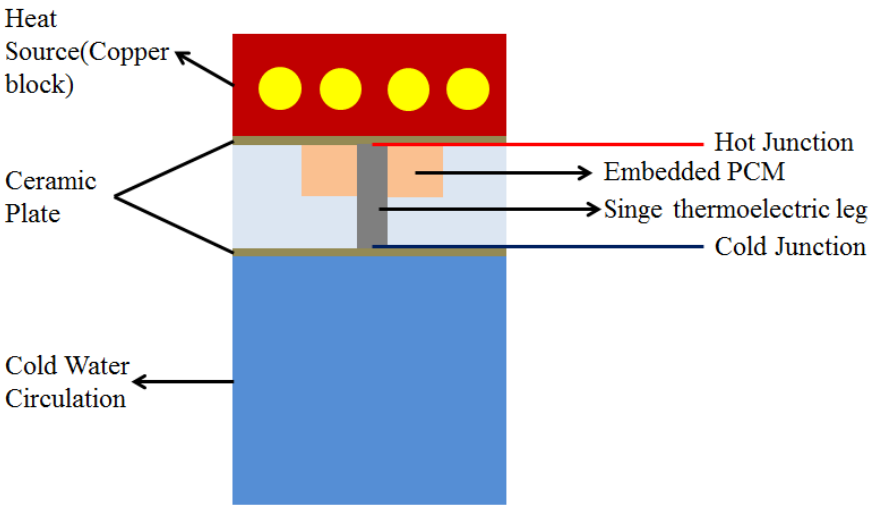

Fig.2. A cross-sectional schematic view of TEM

3.Results and discussion

To discuss the effect of geometrical structure of embedded PCM on the power generation of TEM, two types of TEM (with and without PCM) were used in this study. Type “blank” represents the TEM without PCM. Type “PCM” represents the TEM embedded with different geometrical structure of PCM. For example, the type “d30h8” means the TEM with the PCM stored in a cylindrical space with the diameter of 30 mm and the height of 8 mm.

In group A, the height of PCM is fixed at 8 mm and the cross-sectional diameter is set to be 24, 26, 30 mm. The output voltage variation when the heat source stops supplying heat is shown in Fig. 3. The output voltage of TEM increases with increasing cross-sectional diameter. The maximum output voltage of type “blank” merely reaches 4.0 mV. In the case of type “PCM”, the maximum output voltages are about 0.28-0.56 mV higher than that of type “blank”. The maximum output voltages of type “PCM” increases by magnitude of 7.07-14.15 % compared to that of type “blank”. Maximum output voltage generated by “d30h8” is about 4.5 mV. Besides, the temperature of type “PCM” also holds for 40-60 seconds due to the latent heat stored in the PCM.

The derivative of output voltages and temperature under different diameters varies with time when the heat source stops supplying heat are shown in Fig. 4 and Fig. 5, respectively. In Group A, in the case of type “PCM”, the derivative of output voltages decreases from the maximum to zero within 30s, and then gradually decreases from zero to -0.02 mV/s in the next 70s. The derivative of temperature decreases from the maximum to zero within 30s and

then decrease from zero to -0.15 °C/s in the next 70s. The temperatures and the output voltages maintain the increasing trend within 30s, but the increase rate becomes smaller gradually. The temperature of the hot side increases until it reaches the maximum and then drops stably. The temperature and the output voltage of TEM continue to increase during this time. In addition, in the case of type “blank”, the derivative of output voltages increases from -0.16 to -0.10 mV/s within 30s and then gradually falls to -0.16 mV/s in the next 70s. The derivative of temperature almost keeps unchanging at -0.14. That is, in the case of type “blank”, the temperature decreases continuously when the heat source stops supplying heat. With the increase of the volume of PCMs, more amounts of PCMs can store more heat in the hot side of the TEM. In the case that the heat source stops heating, it makes the decrease rate of hot side temperature of the TEM slow down.

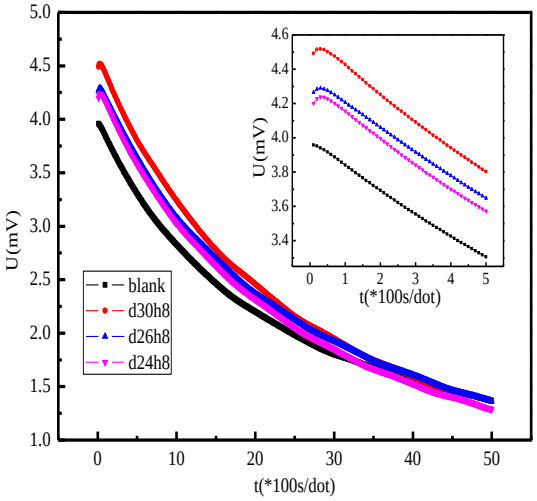

Fig. 3. Group A: Output voltage versus time after the heat source stops heating

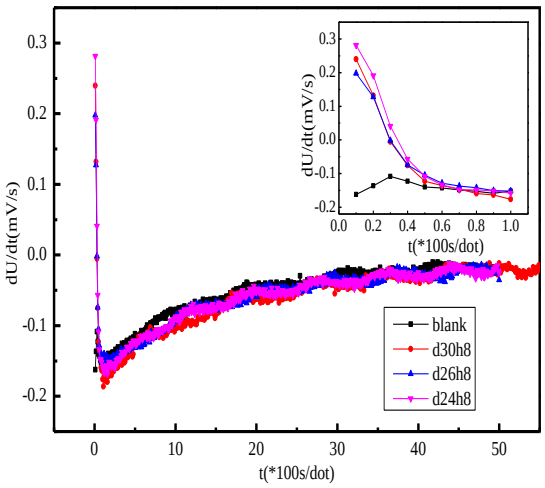

Fig. 4. Group A: The derivative of output voltage varies with time after the heat source stops heating

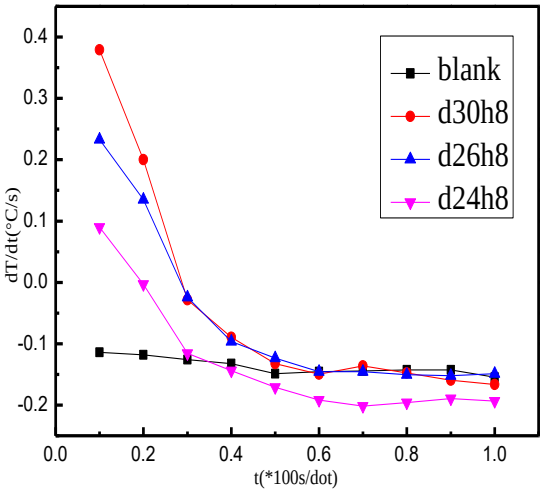

Fig. 5. Group A: The derivative of hot junction temperature varies with time after the heat source stops heating

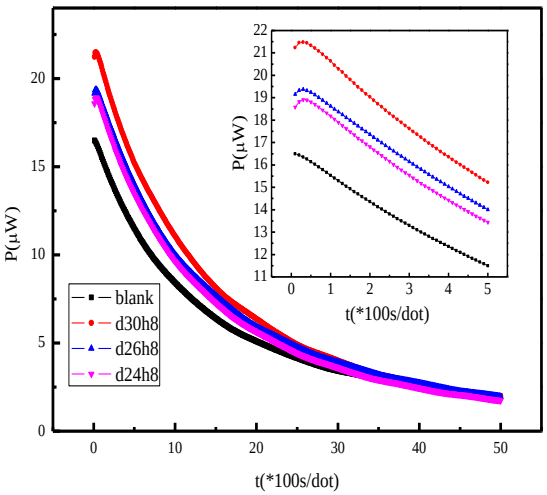

Fig. 6. Group A: Output electrical power variation versus time after the heat source stops heating

The output of TEM was connected to a load resistor with resistance of 0.95 Ω. The time dependence of output electrical power is shown in Fig. 6. The maximum output electrical power of type “blank” merely reaches 16.49 μW. The maximum output electrical power for type “PCM” is about 2.43-5 μW of magnitude higher than that of type “blank”. The maximum output electrical power of type “PCM” increased by about 14.74-30.32 % in comparison of that of type “blank”. Type “d30h8” generates the maximum output electrical power of 21.48 μW.

Tab. 1 presents the comparison between electricity produced by relevant TEM and PCM in group A. In Tab. 1, *m* represents the amounts of PCM calculated according to the relevant parameters mentioned in the above. *W* represents the total electrical energy produced by TEM after the heat source stops supplying heat. The total electrical energy is figured up through integrating output electrical power with time. The TEM with PCM generated more electrical energy compared to the TEM without PCM. Moreover, the conversion efficiency of the TEM with PCM increases with increasing cross-sectional diameter of PCM. The electrical energy of type “blank” is 27.6 mJ. The TEM generates 3-6.9 mJ larger amount of electrical energy than that of TEM without PCM during the whole energy harvest process. The electrical energy of TEM with PCM increases by 10.9-25 % compared to that of TEM without PCM. For the type of “d30h8”, the TEM with 4.3 gram of PCM embedded produces more amount of electricity of about 6.82 mJ than that produced by TEM without the PCM after the heat source stops supplying heat.

Tab. 1. Group A: The comparison between electricity produced by relevant TEM and PCM

	d30h8	d26h8	d24h8	blank
m(g)	4.298	3.228	2.751	0
W(mJ)	34.4242	32.2309	30.551	27.5993

In group B, the cross-sectional diameter of PCM is fixed at 30 mm and the height is set to be 2, 4, 8 mm, respectively. The time dependence of the output voltage is shown in Fig. 7. It can be seen that the temperature of type “PCM” keeps unchanging for 20-60s due to the latent heat stored in the PCM. The output voltage of TEM with PCM increases with the increasing height of PCM. The maximum output voltages of type “PCM” are about 0.3-0.56 mV of magnitude larger than that of type “blank” with the same experimental conditions. The maximum output voltages of type “PCM” increase by 7.58-14.15 % compared with that of type “blank”.

The time dependences of the derivative of output voltages and the temperature after the heat source stops supplying heat are shown in Fig. 8 and Fig. 9, respectively. In Group B, in the case of type “PCM”, the time of the derivative of output voltages decreases from maximum to zero is different. The temperature and output voltages increase with the increasing height of PCM. The derivative of output voltages of type “d30h8” decreases from 0.24 to zero within 30s, while that of the type “d30h4” decreases from 0.044 to zero within 20s. Meanwhile, the derivative of output voltages of type “blank” and type “d30h2” almost keeps constant at -0.15 mV/s. In addition, the time of the derivative of temperature decreases

from the maximum to the stable value of -0.15 °C/s is also different. Since the amount of latent heat stored in the TEM with PCM is different, the increase rates of temperature and output voltage of TEM with PCM are different. Therefore, the type “PCM” also keeps unchanging for different energy harvest time. Fig. 10 shows the time dependence of the output electrical power. The output electrical power of TEM increases with the increasing height of PCM. In the case of type “PCM”, the maximum output electrical power is about 3.4-5 μW of magnitude higher than that of type “blank”. The maximum output voltages of type “PCM” increases by 20.6-30.3 % larger than that of type “blank”.

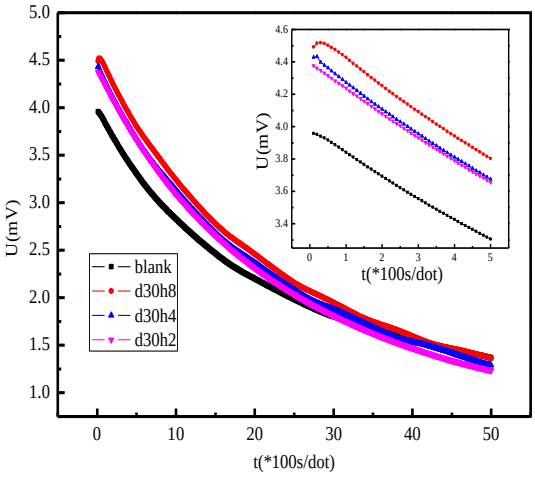

Fig. 7. Group B: Output voltage variation versus time after the heat source stops heating

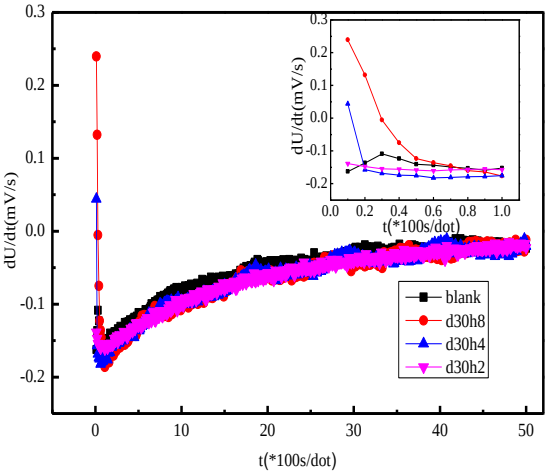

Fig. 8. Group B: The derivative of output voltage varies with time after the heat source stops heating

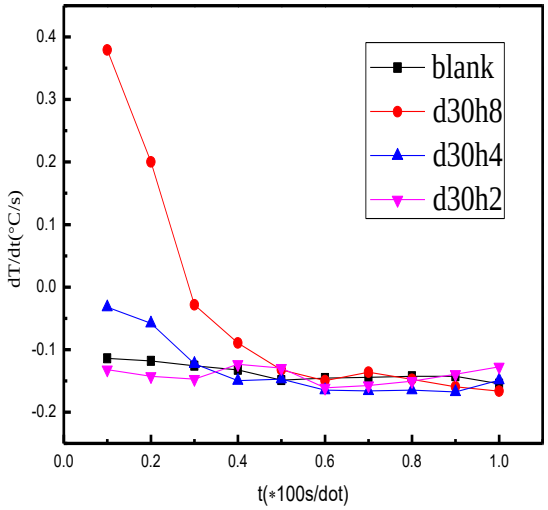

Fig. 9. Group B: The derivative of hot junction temperature varies with time after the heat source stops heating

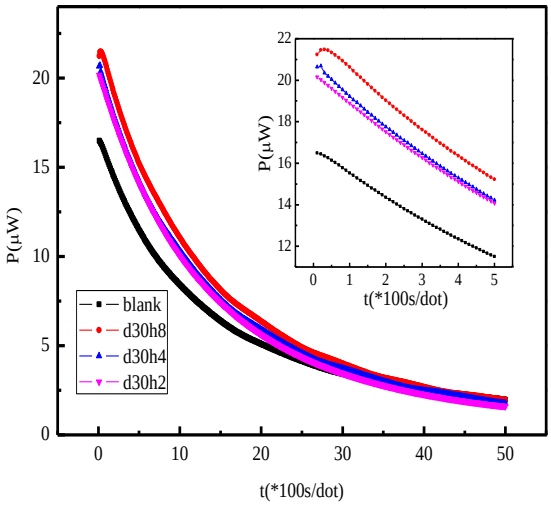

Fig. 10. Group B: Output electrical power variation versus time after the heat source stops heating

Tab. 2 presents the comparison between electricity produced by relevant TEM and PCM in group B. The electrical energy of TEM with PCM embed increases with increasing height of PCM is about 2.6-6.9 mJ of magnitude larger than that of TEM without PCM during

the whole energy harvest process. The electrical energy induced by TEM with PCM is about 9.42-25 % larger than that of TEM without PCM.

The results indicate that the increase of cross-sectional diameter and height of PCM could enhance power generation of TEM with PCM. It is obvious that a larger cross-sectional diameter and a higher height of PCM would increase the amounts of PCM. Therefore, the latent heat storage capacity of PCM can also be increased. When the heat source stops supplying heat, the PCM was used as a heat source. Thus, the hot side temperature of TEM could hold for a period of time. During this period, the TEM with PCM would generate extra electrical energy.

Tab. 2. Group B: The comparison between electricity produced by relevant TEM and PCM

	d30h8	d30h4	d30h2	blank
m(g)	4.298	2.149	1.074	0
W(mJ)	34.4242	32.0093	30.9234	27.5993

4.Conclusion

In this study, the effect of the geometrical structure (the cross-sectional diameter and the height) of embedded PCM on the power generation of fabricated TEM was investigated. It is shown that the TEM with PCM could generate higher output voltage and maintain longer energy harvesting time than that of TEM without PCM, when the heat source stops supplying heat. TEM with 4.3 gram of paraffin wax embed provides 60 seconds longer energy harvesting time and generates 25 % larger of power generation than that of TEM without PCM. In terms of the geometrical structure of embedded PCM, the output voltage and maintained energy harvesting time of TEM with PCM increase with the increasing cross-sectional diameter and height of PCM.

Acknowledgments

This work was supported by the Major Program of the National Natural Science Foundation of China (51590902), the National Natural Science Foundation of China (51476095), and the Program for Professor of Special Appointment (Young Eastern Scholar, QD2015052) at Shanghai Institutions of Higher learning.

References

[1] Klimanek. A, Kostowski. W. J, Burda. G, *et al*. Preliminary design and modelling of a gas-fired thermoelectric generator. *Thermal Science*, 2016, Vol. 20, pp. 1233-1244

[2] B. A. Gupta, S. Chand, N. K. Patel, A. Soni. A review on thermoelectric cooler. *International Journal for Innovative Research in Science & Technology*, 2016, Vol. 2, pp. 674-679

[3] H. J. Goldsmid. Thermoelectric modules and their application. *Introduction to*

Thermoelectricity, 2016, Vol. 121, pp. 197-220

[4] Kumar. R. C, Ankit. S, Rahul. G. Experimental study on waste heat recovery from an internal combustion engine using thermoelectric technology. *Thermal Science*, 2011, Vol. 15, pp. 1011-1022

[5] Y. Zhang, *et al*., High-temperature and high-power-density nanostructured thermoelectric generator for automotive waste heat recovery. *Energy Conversion & Management*, 2015, Vol. 105, pp. 946-950

[6] J. Yang, F. R. Stabler. Automotive applications of thermoelectric materials. *Journal of Electronic Materials*, 2009, Vol. 38, pp. 1245-1251

[7] M. N. Adroja, S. B. Mehta, M. P. Shah. Review of thermoelectricity to improve energy quality. *International Journal of Emerging Technologies and Innovative Research*, 2015, Vol. 2, pp. 847-850

[8] D. Tatarinov, *et al*., Modeling of a thermoelectric generator for thermal energy regeneration in automobiles. *Journal of Electronic Materials*, 2013, Vol. 42, pp.2274-2281

[9] G. Min. Thermoelectric module design under a given thermal input: theory and example. *Journal of Electronic Materials*, 2013, Vol. 42, pp.2239-2242

[10] J. De Boor, E. Müller. Data analysis for seebeck coefficient measurements. *Review of Scientific Instruments*, 2013, Vol. 84, 065102

[11] Saqr. K. M, Musa M. N. Critical review of thermoelectrics in modern power generation applications. *Thermal Science*, 2009, Vol. 13, pp. 165-174

[12] S. Twaha, J. Zhu, Y. Yan, B. Li. A comprehensive review of thermoelectric technology: materials, applications, modelling and performance improvement. *Renewable and Sustainable Energy Reviews*, 2016, Vol. 65, pp. 698-726

[13] Y. Wang, C. Dai, S. Wang. Theoretical analysis of a thermoelectric generator using exhaust gas of vehicles as heat source. *Applied Energy*, 2013, Vol. 112, pp.1171-1180

[14] Yoo. D. W, Joshi. Y. K. Energy efficient thermal management of electronic components using solid-liquid phase change materials. *IEEE Transactions on Device & Materials Reliability*, 2004, Vol. 4, pp. 641-649

[15] D. Samson, T. Otterpohl, M. Kluge, U. Schmid, T. Becker. Aircraft-specific thermoelectric generator module. *Journal of Electronic Materials*, 2009, Vol. 39, pp. 2092-2095

[16] C. K. Yoon, G. Chitnis, B. Ziaie. Impact-triggered thermoelectric power generator using phase change material as a heat source. *Journal of Micromechanics and Microengineering*, 2013, Vol. 23, 114004

[17] S. E. Jo, M. S. Kim, M. K. Kim, Y. J. Kim. Power generation of a thermoelectric generator with phase change materials. *Smart Material Structures*, 2013, Vol. 22, pp. 2870-2876.

[18] A. Elefsiniotis, T. Becker, U. Schmid. Thermoelectric energy harvesting using phase change materials (pcms) in high temperature environments in aircraft. *Journal of Electronic Materials*, 2013, Vol. 43, pp. 1809-1814

[19] A. Agbossou, Q. Zhang, G. Sebald, D. Guyomar. Solar micro-energy harvesting based on thermoelectric and latent heat effects. Part I: Theoretical analysis. *Sensors and Actuators A: Physical*, 2010, Vol. 163, pp. 277-283

[20] Q. Zhang, A. Agbossou, Z. Feng, M. Cosnier. Solar micro-energy harvesting based on thermoelectric and latent heat effects. Part II: Experimental analysis. *Sensors and Actuators A: Physical*, 2010, Vol. 163, pp. 284-290

[21] Q. Zhang, A. Agbossou, Z. Feng, A. C. Grillet. Phase change material and the thermoelectric effect for solar energy harvesting and storage. Proceedings of the asme/jsme 2011 8th thermal engineering joint conference, Hawaii, USA: 2011

[22] X. Q. Wang, A. S. Mujumdar, C. Yap. Effect of orientation for phase change material (pcm) - based heat sinks for transient thermal management of electric components. *International Communications in Heat and Mass Transfer*, 2007, Vol. 34, pp. 801-808